Optical Process Control for extrusion-based Additive Manufacturing methods in construction

Rafay Mohiuddin[1*], Miranda Cruz Policroniades[1*], Martin Slepicka[1*], and André Borrmann[1*]

[1]Chair of Computational Modeling and Simulation, Technical University of Munich, Germany
[*] all authors have contributed equally.

martin.slepicka@tum.de

Abstract -
Additive Manufacturing (AM) provides many advantages when applied to the field of construction. However, due to the large scale of construction projects, time requirements for the printing process are also large, making AM processes susceptible to the influence of external variables. Accordingly, it is advisable to employ methods that can ensure the stability of the extrusion process. This study demonstrates a method to increase the reliability of extrusion-based concrete 3D printing processes through automated monitoring and controlled material extrusion process. In order to maintain a consistent width of the extruded material, a closed-loop optical process control system capable of tracking extruded layers has been developed. It utilizes a mounting system for the monitoring system (RGB camera) that can automatically rotate and moves relative to the printing nozzle and tracks the extruded filament. A computer-vision-based algorithm monitors the filament's width in real-time and continuously transmits the information to a PID controller regulating the material extrusion rate. Overall, the system can effectively track the extruded filament and adjust the extrusion rate based on the vision system, demonstrating significant potential in real-time process control applied in robotic construction.

Keywords -
Digital Fabrication; Automation in Construction; Additive Manufacturing; Process Monitoring; Real time Control, Computer Vision;

1 Introduction

Additive Manufacturing (AM) has been an established technology in many industries for a long time; in particular, it is often used to produce sample components (rapid prototyping). This technology has already revolutionized various industries and shows great potential for the construction industry as it improves construction projects' speed, efficiency, and sustainability [1]. Due to various scaling problems, this technology was not adopted in the construction industry for a long time but is now gaining more acceptance [2]. Many research projects focus on developing new and improved methods and exploring suitable material mixtures.

Another emerging field of research related to AM in construction is the development of appropriate process monitoring systems. Monitoring and progress reporting are essential management functions in delivering construction projects while minimizing delays and cost overruns [3]. The typical workflow for AM with concrete is that the machine control code is created in advance and transmitted to the AM system. Human operators then continuously monitor the corresponding process to intervene in critical deviations.

This type of process control takes a passive approach in which process conditions are initially assumed to be ideal, and recalibration is performed only in response to observed deviations. In addition, deviations can occur at any time that negatively affect, if not completely ruin, the printing process affecting the aesthetics and stability of the component; Even minor deviations can have a critical effect in the further course of the printing process due to superposition effects. Large-scale 3D printing projects, as is common in construction, are also expected to have long production times [2], making the corresponding process monitoring time-consuming and susceptible to human error. In other words, the quality of the printed component hinges on the long-term vigilance, responsiveness, and judgment of the operator.

Thus, an automated monitoring system for AM processes is of high importance. Reliable systems could not only support human supervision but replace it entirely. In this context, and in order to achieve optimal printing results, systems must be developed that can monitor various aspects of the manufacturing process and translate the collected data into suitable feedback signals in near real-time [4].

Computer vision techniques make it possible to monitor the geometry of a component in real-time during the manufacturing process. This work proposes an adaptive control system that can use RGB camera data to regulate the filament width during an extrusion-based concrete 3D print. Contrary to comparable systems, the proposed control methodology is also equipped with a tracking mechanism that can be adapted to different printer configurations and a more precise segmentation method (which also works on a small scale) that can be calibrated for different materials and lighting conditions.

2 Background

AM, also known as 3D printing, generally describes a manufacturing principle in which an object is created based on a digital model by applying or binding material layer by layer using a robotic actuator. According to this principle, methods capable of processing concrete, steel, and wood have been developed for the construction industry. In fact, for these materials, various methods have been developed that can be categorized according to the type of material application, i.e., deposition or particle bed methods [2]. For the present study, concrete printing processes by material deposition are particularly important.

2.1 Concrete 3D printing by material deposition

In concrete printing methods by means of deposition, often also referred to as extrusion-based methods, the cementitious material is deposited layer by layer in a continuous filament through a nozzle [5]. Different variants of this technique vary in nozzle shape and guidance [6, 2, 7] but also in the strategy with which the material is deposited. P. Carneau et al. [8] distinguish between "infinite brick", free flow, and layer pressing strategy (cf. Fig. 1). In addition, the material composition is of great importance [9, 10, 11].

To achieve an optimum print result, it is important that all the previously mentioned parameters are attuned to each other. Among these parameters, properties of material used for printing are most susceptible to variation of the external conditions, introduced by longer printing time. It is to be noted that AM processes for large-scale projects take a considerable time to complete. Any deviation in material properties over time can either result in under-extrusion (tearing) or over-extrusion (buckling) of the material (cf. Fig. 2) [7]. This not only reduce the quality of the print but also makes the structure unstable when consecutive layers are added.

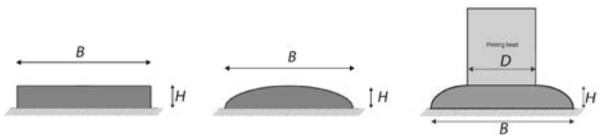

Figure 1. Different concrete extrusion strategies. From left to right: "infinite brick", free flow, and layer pressing strategy [8]

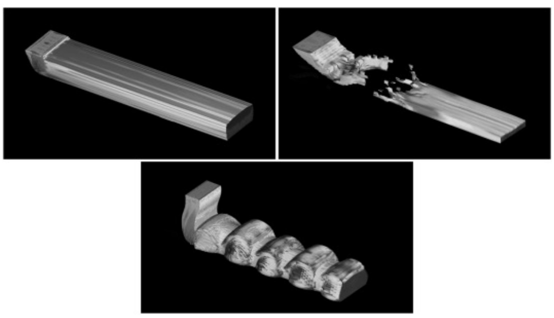

Figure 2. Filament integrity: ideal (left), tearing (right), and buckling (bottom) [7]

2.2 Process control

One solution to stabilize the process is to use an extrusion force-velocity controller [12]. The thickness of the extruded filament depends on how much material is deposited at a particular instant. This can be controlled by adjusting the robot speed (speed of print nozzle) or the extruder speed (material extrusion rate). Advanced methods like synchronization between extrusion and robot speed [13] and model-aware control [14] can make the extrusion process even more reliable.

Another approach is to actively measure the extruded filament's dimension and correct the extrusion process's speed to get the desired dimension. This approach thus consists of two tasks, dimension monitoring on the one hand and extrusion control on the other. For the first task, current advances in computer vision technology make it possible to measure dimensions with ordinary cameras effectively. For the second task, a control loop feedback mechanism can be employed. A commonly used controller is the so-called proportional-integral-derivative (PID) controller, which constantly calculates an error term (difference between measured and nominal value of the control variable) and determines a control value by utilizing proportional, integral and derivative terms [15].

Kazemian et al. [16] proposed a solution to measure the dimension of an extruded filament using a 720p web camera in their study. One of the features of their dimension measurement system is that it averages the measurement over a specified time, which allows them to reduce noise in the measured value. Based on the obtained camera data, a proportional controller then corrects the material extrusion rate (volume flow) by adjusting the speed of the extruder.

Similarly, Shojaei Barjuei et al. [17] proposed a methodology for dimension measurement based on edge detection in their study. Instead of averaging camera-based measurements, their approach used the real-time data feed of an industrial camera with a high frame rate directly for their control system. Via a PI controller, this data was used to control the speed of the AM robot (printing head), to adjust the rate of material deposition. Both of these systems were tested on industrial robots for a large-scale system, which was demonstrated by controlled material extrusion in a straight line.

In another study, Wolfs et al. [18] proposed to use a precise laser line profiler for the dimension measurement. They developed a clash control system that compares point cloud data with the "as-planned" geometry to control the printing process.

In the present study, a near real-time optical process control system was developed and tested on a scaled-down 3D printing setup consisting of a 6-DOF robotic manipulator with a fixed (non-rotating) round nozzle configuration.

A separate rotating head was developed that automatically orientates an RGB camera along the extruded filament using "as-planned" fabrication information. A Computer-vision-based algorithm is then employed to dynamically track and determine the extruded filament's width. A closed-loop feedback control utilizes the measured dimension, determined at every frame from the camera, and evaluates a correction value using a PID controller. Based on the correction value from the controller, the material extrusion rate is adjusted. In contrast to the relevant studies [16, 17, 18], key differences of the proposed method are the printing configuration, synchronization of robot **and** printer, as well as the employed computer vision algorithm. The small scale of the print, combined with the unclear edges due to the layer-pressing strategy of the print and the fixed nozzle configuration, required some adaptations compared to the other systems.

3 Equipment setup

A small-scale experimental setup was used for testing, as illustrated schematically in Fig. 3. The individual components are described in detail in the following sections.

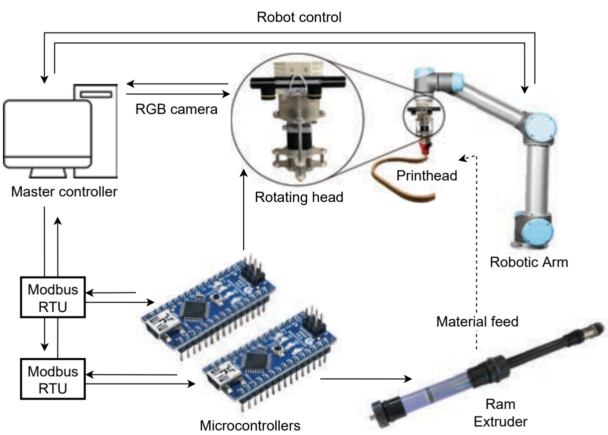

Figure 3. Experimental setup architecture

3.1 Robot/Hardware communication

The main component of the setup is a Universal Robot UR10e robotic arm with 6 degrees of freedom (DoF), which operates independently of a 1.5L ram extruder. The ram extruder conveys the material through a build-up pressure generated by a stepper motor. Once the motor is activated, the material is pumped via a tube toward the printhead. At the printhead, a second stepper motor operates an auger screw, which finally extrudes the material through the nozzle. The stepper motors are controlled by the master controller via a microcontroller using the serial transmission protocol, Modbus RTU.

The robot movement is currently programmed offline and manually transmitted to the robot as an URscript file. During execution, the velocity can variate or remain stable depending on the geometry. The print information is transmitted per TCP/IP connection to the master controller using the so-called RTDE interface (Real Time Data Exchange) provided by UR.

3.2 Printhead

The printhead is outfitted with a round nozzle with which the material can be deposited utilizing the layer-pressing strategy. Due to the material intake, i.e., the tube between the printhead and the ram extruder, the freedom of movement of the robot is limited to 5 DoF, the sixth axis must not be rotated. However, since the relative orientation of the filament to the printhead can change during the process depending on the geometry, the field of view of a camera mounted directly on the printhead would be very limited. To increase the field of view, a camera mount was developed that can rotate around the printhead independently of the robot's motion (cf. Fig. 3). A second microcontroller was installed for controlling the rotating camera mount, which is also connected via a serial link using Modbus RTU.

3.3 Camera

For the optical monitoring task of the proposed process control system, an RGBD camera (ZED mini) was installed on the rotating camera mount. Although the camera can be used for depth measurements, only one of the camera's lenses was used, effectively downgrading the monitoring system to a simple RGB camera. During the printing process the camera is set up to transmit a continuous 720p video feed.

4 Methodology

4.1 Optical process monitoring

The objective of the monitoring system is to measure the width of the extruded filament. To realize this, the image frames of the camera's video feed are processed utilizing computer vision algorithms to extract the filament width.

The approach used for image processing is similar to the method proposed by Kazemain et al. [16]. The key difference is the segmentation method (separating target object from surrounding) and utilization of all frames (60 frames per second) instead of sampling for more accuracy, in order to decrease the reaction time of the control system, making the system more reliable in highly dynamic processes [17]. For segmentation, a mask is created based on HSV (hue saturation value), and the value range for HSV value is adjusted manually using track bars (cf. Fig. 4). The value of the range predominantly depends on the background and luminous intensity.

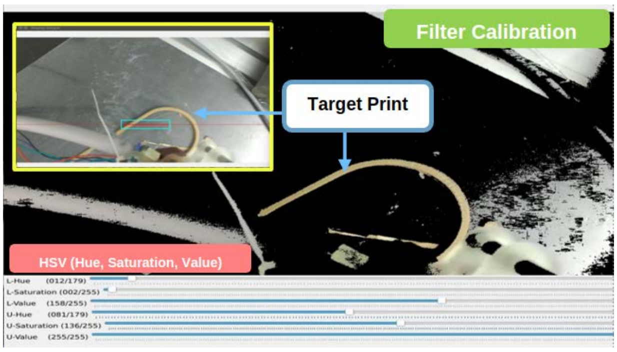

Figure 4. GUI for calibrating HSV range values

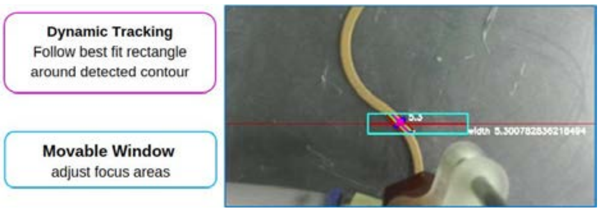

Figure 5. Contour tracking by estimating rectangle with smallest area over detected contour in focus area.

As illustrated in Fig. 5, only a small cropped segment of every image frame focusing the region around the target object (printed filament) is used for the width detection. The position of this cropping rectangle is set manually. It should be chosen as small as possible to minimize noise but large enough so that the filament can be detected even if the camera mount is rotated imprecisely. Cropping the image speeds up the computation time by reducing the number of pixels and the probability of noise.

HSV-based segmentation mask is then applied to the cropped frame to separate the target object from its surrounding. The HSV-based method mainly relies on the difference in color gradient between the background and printed material and thus can be made flexible for intensity value making it less prone to erroneous measurement because of lighting conditions. On each frame with the segmented object, the full family of contours is retrieved in a hierarchical list, including all boundary points of the contour [19]. All contours of each individual frame are filtered based on the minimum pixel area to prevent any unnecessary noise. The minimum pixel area of a contour is another hyperparameter along with the HSV value range. It addresses the sensitivity of the monitoring system as it limits the minimum size that can be detected. In the last step, the dimension is measured by converting the pixel width of the rectangle to centimeters.

For all the presented steps, a calibration must first be performed once when the system is set up or exterior influences change (e.g., lighting). In order to make this more convenient, a user interface (UI) has been implemented that can be called when necessary, providing:

- **Scaling (pixels per cm):** User input prompt requiring a calibration measurement of an object with known dimensions. It takes the correct measurement as input and calculates the scaling factor.
- **Movable Window:** Sliders allow the user to adjust the position and size of the focus area (cf. fig. 5) by moving two corner points in relation to the center of the image.
- **HSV Calibration:** The user can adjust maximum and minimum HSV-values and thus the upper (U) and lower (L) segmentation thresholds. The values must be adjusted until only the specimen is visible (cf. fig. 4).

4.2 Process control

Once a printing process is started on the UR10e robot controller, the process control algorithm (Main controller, cf. Fig. 6) obtains input from the robot via its RTDE interface. In parallel, the camera provides a continuous video feed to the main controller. As soon as the printed filament is detected on any video frame and its width is measured (skipping the first 20 valid frames for good measure), the PID controller (part of the main controller) is enabled. The PID controller returns a cumulative term that is to be added to the extrusion speed as a correction value. The calculated extrusion speed (adapted to the current robot speed) and the PID value are continuously transmitted to Microcontroller 1, which controls the ram extruder and the print head (cf. Fig. 6).

In parallel to the optical process control, a second microcontroller is employed to control the camera position via the rotating mounting system. This system ensures that the focus area of the camera (cropping rectangle, cf. Section 4.1) is centered on the filament. The necessary rotation angle is calculated using the current and two previous waypoint positions of the robot and sent to

Microcontroller 2 (cf. Fig. 6, see also section 4.4). Microcontroller 2 controls the motor of the camera mount and adapts the position accordingly. In contrast to the extrusion speed, this process only occurs at each waypoint change and terminates once the position is reached.

The process control is terminated once the final waypoint is detected.

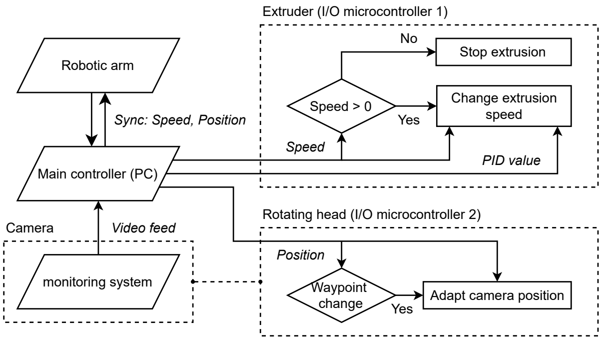

Figure 6. Optical process control monitoring system execution flowchart

4.3 Robot data exchange

As discussed above, a pivotal point for online monitoring is the robot data exchange (current speed and position). Via the UR robots Real-Time Data Exchange (RTDE) interface, it is possible to continuously exchange data between the robot and a computer using a TCP/IP connection. The update rate of this data exchange can be set to up to 500 Hz. Also, the interface is able to skip packages in case of any process holdups so that always the most recent data is exchanged. During the printing process, a constant RTDE feed between the robot and the main controller (PC, cf. Fig. 6) is maintained.

4.4 Rotating head

As mentioned in section 3.2, the system proposed in this study was developed for a 5-DoF system (limitation due to the used print head). Due to the fixed sixth robot axis, a camera mounted directly on the printhead would be limited in its field of view to only one direction. However, since arbitrary geometries can be printed with the AM system, it is necessary to integrate a dynamic camera mount into the monitoring system. For this purpose, a rotating camera mount was implemented that is controlled using the mentioned RTDE position updates from the robot. As the robot path is known in advance (defined by the component's geometry), waypoints for camera position updates can also be defined in advance. Every time the robot gets close enough to such a waypoint a signal is sent to the respective microcontroller which then initiates a position change. From the current position the last three waypoints (A, B, C) are considered for the calculation of the rotation angle. Between these three points, it is possible to calculate an angle by calculating the slopes (m_1 and m_2) of the lines $\overline{AB}$ and $\overline{BC}$ and solving equation 1 to θ.

$$\tan\theta = \frac{m_1 - m_2}{1 + (m_1 \cdot m_2)} \tag{1}$$

The result is translated into motor steps and direction and sent via Modbus RTU to Microcontroller 2 controlling the camera mount (cf. Fig. 3 and 6). This function runs independently of the extrusion speed and is only executed when needed. The Modbus protocol allows each microcontroller to work simultaneously or independently from the other.

4.5 Extrusion speed

The extrusion speed is calculated using the sync speed as the main parameter. By formulating a relation between the extruder motor speed and the robot's actual speed, the extrusion rate ($Q_{extruder}$) can be synchronized with the filament deposition rate ($Q_{filament}$):

$$Q_{extruder}\left[\frac{mm^3}{s}\right] = Q_{filament}\left[\frac{mm^3}{s}\right] \tag{2}$$

On the right side of equation 2, the filament deposition rate is calculated with equation 3 using the user input parameters, filament width (d_f) and the layer height (h_l) which are unique to the setup and the geometry, and actual robot speed (v_{TCP}), i.e. the Tool Center Point (TCP) movement speed obtained via the RTDE interface (cf. section 4.3). It should be noted that the equation 3 is based on the assumption that the filament has a rectangular shape, which is not exactly the case with the layer pressing strategy [8]. The inaccuracy acts as a constant factor, which is, however, compensated for by the proposed PID controller (cf. section 4.6) and is therefore negligible.

$$Q_{filament} = v_{TCP}\left[\frac{mm}{s}\right] \cdot d_f\,[mm] \cdot h_l\,[mm] \tag{3}$$

On the left side of equation 2, the extrusion rate is based on the extruder setup. When a mechanical conveying system powered by a stepper motor is employed, as is the case in this study, the extrusion rate can be expressed as the product of the turn frequency f_{motor} of the motor and a specific volume flow q_{ram} defined by the extruder geometry (cf. equation 4).

$$Q_{extruder} = f_{motor}\left[\frac{step}{s}\right] \cdot q_{ram}\left[\frac{mm^3}{step}\right] \tag{4}$$

By using equations 4, 3 and 4 and by solving to f_{motor} it can be derived that the motor speed of the ram extruder is linear proportional to the filament width (d_f). Due to that fact, a PID controller can be used to control the extrusion rate when monitoring the filament width.

4.6 PID controller

As mentioned before, a PID controller was chosen as the control architecture for the optical process control system proposed in this paper. The controller calculates the error term e as the difference between the measured "as-manufactured" filament width and the "as-designed" width. With this error value e, the PID output $u(t)$ is calculated via equation 5.

$$u(t) = K_P e(t) + K_i \int e(t)dt + K_P \frac{de}{dt} \quad (5)$$

In equation 5, the frame rate of the camera is used as the time domain to avoid conversions. Using the equations 2, 3 and 4, the calculated PID value $u(t)$ can finally be converted into a motor frequency f_{PID}, which is transferred to the extruder controller (microcontroller 1, see Fig. 6) as a correction value. Since every frame is processed during monitoring (see section 4.1), additionally a failsafe was implemented in case incorrect values were determined, e.g. due to noise. With a simple threshold value procedure, measured values that are too small or too large are simply discarded and the unregulated motor frequency is used as the control variable (cf. Fig. 7).

The PID tuning – setting of the PID constants K_P, K_I and K_D – was performed utilizing several test prints of a very simple geometry, a single straight line (cf. [15]). The measured data for each individual test print were plotted and examined for their convergence behavior. Depending on the behavior, the PID factors were then adjusted accordingly, first the K_P value, then K_D and finally K_I. The tuning outcome setting for our system is (K_P = 20), (K_D = 1) and (K_I = 0.01).

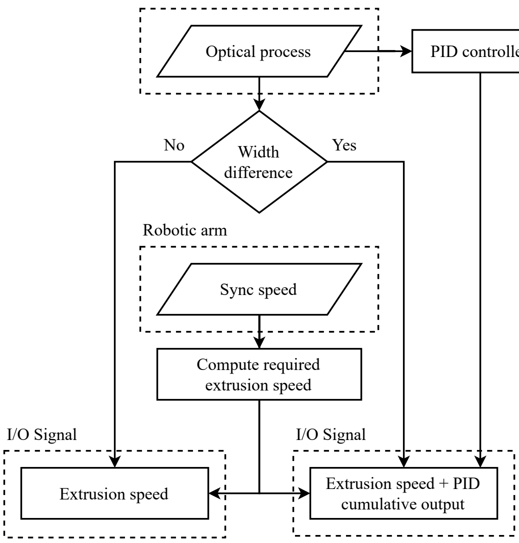

Figure 7. Data exchange for extrusion speed control.

5 Experimental validation

To evaluate the performance of the proposed optical process control, a small scale clay 3D printing setup was used printing along a curved print path. For the first run, the camera and the rotating head algorithm were activated to be able to observe the width of the extruded material, but the PID extruder control was disabled (cf. Fig. 8, left). In the second run, the complete optical process control, including PID, was activated (cf. Fig. 8, right). The initial configuration was set to be the same as in the first run. The expected filament width for both experiments was $6mm$.

As a result of an uneven print bed, the uncontrolled 3D print produced a filament with variable filament width. Additionally, with the used setup, an exact initial configuration of the nozzle height is not possible. As illustrated in Fig. 8, both of these issues accumulate to a clearly visible error in the filament width – the width is not constant and with a value of around $12mm$, depending on the position, too large.

As illustrated in Fig. 8, right, the developed process control applied in the same setup is not only able to detect the changes of the filament throughout the print, but it is also able to update the control value correctly, maintaining a filament width of close to $6mm$. The results of this experiment demonstrate the potential of our process control as it provides automatic supervision and in-time corrections during the printing process. Further improvements to the system are discussed in the following section.

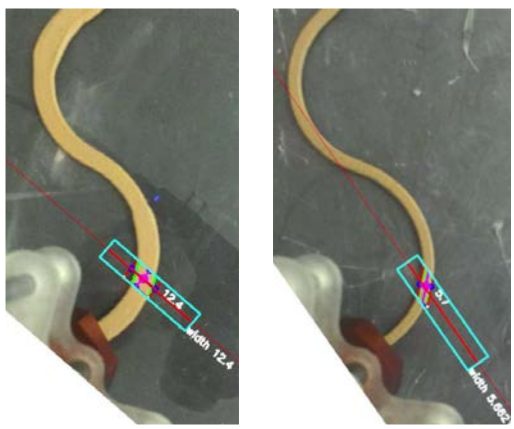

Figure 8. Test print using a curved print path: uncontrolled (left) and controlled (right).

6 Limitations and future work

One of the limitations of the proposed system is tracking sharp curves with small angles of rotation. By reducing this distance between printhead and camera, it will be possible to track and test such complex geometries. Reducing distance to the printhead will also reduce the distance between the nozzle and the camera objective. As visible in Fig. 8, there is a lag of information between what is being printed and what is being measured. The implemented PID helps regulate this disturbance but reducing this distance with a different camera mount could improve the efficiency of the system.

If multiple layers are being printed and in the case of under extrusion with very little difference between the current and previous layer, HSV based filters might ignore the current layer and return the measurement of previous layer. This can be avoided by using depth based filters. However, a RGBD camera cannot sufficiently resolve depth at such small scales. Alternatively, for a small scale experimental setup, laser profilers that provide a much larger resolution can be used, as proposed by Wolfs et al. [18].

The implemented HSV-based segmentation performs more reliable compared to the noisy measurements of the segmentation method proposed in [16], but in the current state of the implementation it relies on manual calibration. To limit the need for manual calibration, automatic thresholding techniques and methods like mask RNN can be explored in detail for automated segmentation, making the vision system completely independent of external environmental variables. An automated calibration process can help get rid of the user-induced error but a reference still needs to be set when using HSV. For instance, the material color might not always be the same and this will still have to be adjusted manually.

For the experimental validation, a small-scale clay 3D printing setup was used. While the developed process control system is in principle applicable to any scale of additive manufacturing, an experimental proof for larger scales and other materials (concrete) has not yet been performed. This is subject to future work.

7 Conclusion

In this paper, a methodology to increase the reliability of additive manufacturing process in the field of construction, through automated monitoring and controlled material extrusion process has been introduced. In order to maintain a consistent width of the extruded material, a closed loop optical process control system capable of tracking the extruded filament has been developed. It utilizes an independent rotating head for a camera that moves relative to the nozzle and tracks the extruded filament. A computer-vision based algorithm, monitors the width of the filament in real time, which is then used to regulate the material extrusion rate using a PID controller. Overall, the system is able to effectively track the path and adjust the extrusion rate based on a simple RGB vision system and demonstrates great potential in the area of real-time process control applied in robotic construction. In particular, it provides the basis for implementing the comprehensive concept of cyber-physical production systems in construction.

In contrast to the previous studies mentioned in section 2.2 the proposed control system was able to perform reliable even on a small-scale – the segmentation methods proposed in the previous studies resulted in a noisy measurement of the print path. It was shown that with a 1920x1080 px resolution camera with 60 fps satisfactory control was obtained without averaging frames, mainly because of the difference in segmentation method. Additionally, the control system represents a novel approach for use with extruder systems that have a fixed printing nozzle (layer pressing strategy), where an additional filament tracking system is required.

Acknowledgments

The research presented is part of the Transregio 277 'Additive Manufacturing in Construction – The Challenge of Large Scale', funded by the Deutsche Forschungsgemeinschaft (DFG, German Research Foundation) – project number 414265976 – TRR 277.

References

[1] Seyed Hamidreza Ghaffar, Jorge Corker, and Mizi Fan. Additive manufacturing technology and its implementation in construction as an eco-innovative solution. *Automation in Construction*, 93:1–11, September 2018. doi:10.1016/j.autcon.2018.05.005. URL `https://doi.org/10.1016/j.autcon.2018.05.005`.

[2] Alexander Paolini, Stefan Kollmannsberger, and Ernst Rank. Additive manufacturing in construction: A review on processes, applications, and digital planning methods. *Additive Manufacturing*, 30, 12 2019. ISSN 22148604. doi:10.1016/j.addma.2019.100894.

[3] D Shamsollahia, O Moselhib, and K Khorasanic. Construction progress monitoring and reporting using computer vision techniques–a review. *39th International Symposium on Automation and Robotics in Construction (ISARC 2022)*, pages 467–472, 2022.

[4] Rob JM Wolfs, Freek P Bos, Emiel CF van Strien, and Theo AM Salet. A real-time height measurement and feedback system for 3d concrete printing. In *High*

Tech Concrete: Where Technology and Engineering Meet, pages 2474–2483. Springer, 2018.

[5] Manu K. Mohan, A.V. Rahul, Geert De Schutter, and Kim Van Tittelboom. Extrusion-based concrete 3d printing from a material perspective: A state-of-the-art review. *Cement and Concrete Composites*, 115:103855, 2021. ISSN 0958-9465. doi:https://doi.org/10.1016/j.cemconcomp.2020.103855. URL https://www.sciencedirect.com/science/article/pii/S0958946520303607.

[6] Xiangpeng Cao, Shiheng Yu, Hongzhi Cui, and Zongjin Li. 3d printing devices and reinforcing techniques for extruded cement-based materials: A review. *Buildings*, 12(4):453, April 2022. doi:10.3390/buildings12040453. URL https://doi.org/10.3390/buildings12040453.

[7] R.J.M. Wolfs, T.A.M. Salet, and N. Roussel. Filament geometry control in extrusion-based additive manufacturing of concrete: The good, the bad and the ugly. *Cement and Concrete Research*, 150:106615, December 2021. doi:10.1016/j.cemconres.2021.106615. URL https://doi.org/10.1016/j.cemconres.2021.106615.

[8] Paul Carneau, Romain Mesnil, Nicolas Ducoulombier, Nicolas Roussel, and Olivier Baverel. Characterisation of the Layer Pressing Strategy for Concrete 3D Printing. In Freek P. Bos, Sandra S. Lucas, Rob J.M. Wolfs, and Theo A.M. Salet, editors, *Second RILEM International Conference on Concrete and Digital Fabrication*, pages 185–195, Cham, 2020. Springer International Publishing. ISBN 978-3-030-49916-7.

[9] Rjm Rob Wolfs, Freek P. Bos, and Tam Theo Salet. Early age mechanical behaviour of 3d printed concrete: Numerical modelling and experimental testing. *Cement and Concrete Research*, 106:103–116, 2018.

[10] A. Perrot, D. Rangeard, and A. Pierre. Structural built-up of cement-based materials used for 3d-printing extrusion techniques. *Materials and Structures*, 49(4):1213–1220, February 2015. doi:10.1617/s11527-015-0571-0. URL https://doi.org/10.1617/s11527-015-0571-0.

[11] A.S.J. Suiker. Mechanical performance of wall structures in 3d printing processes: Theory, design tools and experiments. *International Journal of Mechanical Sciences*, 137:145–170, March 2018. doi:10.1016/j.ijmecsci.2018.01.010. URL https://doi.org/10.1016/j.ijmecsci.2018.01.010.

[12] Bradley K. Deuser, Lie Tang, Robert G. Landers, Ming C. Leu, and Greg E. Hilmas. Hybrid extrusion force-velocity control using freeze-form extrusion fabrication for functionally graded material parts. *Journal of Manufacturing Science and Engineering*, 135(4), July 2013. doi:10.1115/1.4024534. URL https://doi.org/10.1115/1.4024534.

[13] Pinyi Wu, Keval S. Ramani, and Chinedum E. Okwudire. Accurate linear and nonlinear model-based feedforward deposition control for material extrusion additive manufacturing. *Additive Manufacturing*, 48:102389, December 2021. doi:10.1016/j.addma.2021.102389. URL https://doi.org/10.1016/j.addma.2021.102389.

[14] Hesam Zomorodi and Robert G. Landers. Extrusion based additive manufacturing using explicit model predictive control. In *2016 American Control Conference (ACC)*. IEEE, July 2016. doi:10.1109/acc.2016.7525169. URL https://doi.org/10.1109/acc.2016.7525169.

[15] Pid controller explained, n.D. URL https://pidexplained.com/pid-controller-explained/.

[16] Ali Kazemian, Xiao Yuan, Omid Davtalab, and Behrokh Khoshnevis. Computer vision for real-time extrusion quality monitoring and control in robotic construction. *Automation in Construction*, 101:92–98, 5 2019. ISSN 09265805. doi:10.1016/j.autcon.2019.01.022.

[17] E. Shojaei Barjuei, E. Courteille, D. Rangeard, F. Marie, and A. Perrot. Real-time vision-based control of industrial manipulators for layer-width setting in concrete 3d printing applications. *Advances in Industrial and Manufacturing Engineering*, 5, 11 2022. ISSN 26669129. doi:10.1016/j.aime.2022.100094.

[18] Rob J.M. Wolfs, Freek P. Bos, Emiel C.F. Van Strien, and Theo A.M. Salet. A real-time height measurement and feedback system for 3d concrete printing. In *High Tech Concrete: Where Technology and Engineering Meet*, pages 2474–2483. fib. The International Federation for Structural Concrete, 2018. ISBN 9783319594705. doi:10.1007/978-3-319-59471-2_282.

[19] Opencv contours documentation, 2022. URL https://docs.opencv.org/3.4/d3/d05/tutorial_py_table_of_contents_contours.html.